Langenbeck's Archives of Surgery (2024) 409:124
https://doi.org/10.1007/s00423-024-03318-8

RESEARCH

The mesenteric entry site as a potential weak point in gastrointestinal anastomoses – findings from an *ex-vivo* biomechanical analysis

Kamacay Cira[1] · Saskia Nicole Janett[1] · Carina Micheler[2,3] · Stephan Heller[2] · Andreas Obermeier[2] · Helmut Friess[1] · Rainer Burgkart[2] · Philipp-Alexander Neumann[1]

Received: 3 March 2024 / Accepted: 8 April 2024

Abstract

Purpose Gastrointestinal disorders frequently necessitate surgery involving intestinal resection and anastomosis formation, potentially leading to severe complications like anastomotic leakage (AL) which is associated with increased morbidity, mortality, and adverse oncologic outcomes. While extensive research has explored the biology of anastomotic healing, there is limited understanding of the biomechanical properties of gastrointestinal anastomoses, which was aimed to be unraveled in this study.

Methods An *ex-vivo* model was developed for the biomechanical analysis of 32 handsewn porcine end-to-end anastomoses, using interrupted and continuous suture techniques subjected to different flow models. While multiple cameras captured different angles of the anastomosis, comprehensive data recording of pressure, time, and temperature was performed simultaneously. Special focus was laid on monitoring time, location and pressure of anastomotic leakage (LP) and bursting pressures (BP) depending on suture techniques and flow models.

Results Significant differences in LP, BP, and time intervals were observed based on the flow model but not on the suture techniques applied. Interestingly, anastomoses at the insertion site of the mesentery exhibited significantly higher rates of leakage and bursting compared to other sections of the anastomosis.

Conclusion The developed *ex-vivo* model facilitated comparable, reproducible, and user-independent biomechanical analyses. Assessing biomechanical properties of anastomoses offers an advantage in identifying technical weak points to refine surgical techniques, potentially reducing complications like AL. The results indicate that mesenteric insertion serves as a potential weak spot for AL, warranting further investigations and refinements in surgical techniques to optimize outcomes in this critical area of anastomotic procedures.

Keywords Anastomotic leakage · Biomechanics · Anastomosis · Mesentery · Bursting pressure

Introduction

Anastomotic leakage (AL) is still a significant complication [1–13] that can lead to severe infections and even life-threatening sepsis [14, 15]. Despite ongoing advancements in surgical techniques and perioperative treatments, AL presents with varying rates depending on the location of the intestinal anastomosis with up to 19.5% [6, 12] in the upper gastrointestinal tract and up to 25.6% in the lower gastrointestinal tract [3, 5, 7]. Resulting mortality rates range from 4.3% to 43.8% [6, 16–18]. Furthermore AL has been linked to local [19] and distant tumor recurrence [20] in patients with gastrointestinal malignancies. AL causes not only significant personal suffering for patients but also substantial economic challenges for healthcare systems [21].

Rainer Burgkart and Philipp-Alexander Neumann shared Authorship.

✉ Philipp-Alexander Neumann
P-A.Neumann@tum.de

[1] Department of Surgery, Klinikum Rechts Der Isar, TUM School of Medicine and Health, Technical University of Munich, 81675 Munich, Bavaria, Germany

[2] Department of Orthopaedics and Sports Orthopaedics, Klinikum Rechts Der Isar, TUM School of Medicine and Health, Technical University of Munich, Munich, Germany

[3] Institute for Machine Tools and Industrial Management, TUM School of Engineering and Design, Technical University of Munich, Munich, Germany

Published online: 13 April 2024

Therefore, it is not surprising that investigation of anastomotic healing and prevention of AL have been of central importance in surgical research to date. Risk factors for AL can be broadly classified into surgical-related and patient-related factors. The former encompasses errors in surgical techniques, such as anastomosis under tension, inadequate anastomotic perfusion, and suboptimal technique, both in the context of laparoscopic and open surgery. Additional considerations involve the timing of surgery, surgeon experience, and the choice between hand-sewn or stapled procedures, as well as the anastomotic level or the use of a protective stoma. On the other hand, patient-related factors present a distinct set of considerations, including obesity, malignancy, poor nutritional status, smoking, blood loss, chemoradiotherapy, and the composition of the gut microbiome [22, 23]. Understanding the interplay between these factors is crucial for comprehensive risk assessment and effective prevention strategies in the context of anastomotic healing. While these categorizations offer a comprehensive overview of various risk factors associated with AL, it is crucial to underscore the significance of biomechanical studies.

The biomechanical intricacies of anastomoses play a pivotal role in the healing process. A profound comprehension of how mechanical forces, suture techniques, and anatomical considerations interact is imperative for successful outcomes. Without meticulous attention to these biomechanical aspects, an environment conducive to adequate wound healing during and after surgery cannot be established. Indeed, the effectiveness of prevention strategies and the overall success of anastomotic procedures hinge upon the surgeon's ability to apply sound biomechanical principles during and after surgery. The selection of appropriate suture techniques, consideration of mechanical stress, and the careful evaluation of anatomical vulnerabilities are integral components of this biomechanical understanding. Biomechanical studies involve quantitative measurements of factors such as bursting pressure (BP), tensile strength, suture holding capacity, and other mechanical properties and provide valuable insights into identifying potential risk factors, developing preventive strategies, and aiding surgeons in making informed decisions on anastomotic technique [24–27].

The objective of this study was to investigate the biomechanical properties of gastrointestinal anastomoses, with a specific emphasis on analyzing the time, location, and pressure of leakage and bursting. The aim was twofold: firstly, to identify technical weak points within the anastomosis, and secondly, to assess whether variations in suture techniques and flow models would influence these weak points. This was achieved through a comprehensive *ex-vivo* test setup, specifically developed for this study.

Materials and methods

Chemicals and consumable materials

A detailed list of used chemicals, reagents, parent solutions, surgical and consumable material can be found in Supplementary Table 1.

Biologic material – porcine small intestine

The resemblance between porcine small intestine and its human counterpart, both at microscopic and macroscopic levels, has been well-documented in prior research [28, 29]. Thus, for all experiments conducted in this study, porcine small intestine was selected for anastomosis formation. The choice of the origin of the tissue utilized in the experiments was guided by ethical considerations, including 3 R principles for reduction, replacement and refinement of animal experiments [30]. Thus the porcine small intestine was obtained from the Center of Preclinical Research affiliated with the Klinikum rechts der Isar of the Technical University of Munich. Therefore, the utilization of animal products in this study solely relied on byproducts from animals already sacrificed for other experimental purposes, eliminating the need to sacrifice additional animals specifically for the experimental purpose in this study.

The porcine small intestine was obtained promptly after the scarification of the animals and underwent a thorough cleaning process using water before being utilized. To counteract the potential adverse effects of tissue degeneration on experimental outcomes, the harvested tissue was stored in a refrigerator, maintained at a temperature of 4 degrees Celsius (°C), and kept moisturized for a maximum of 12 h.

Ex-vivo model for evaluation of stability and pressure resistance of gastrointestinal anastomoses

The *ex-vivo* test setup consists of five main components: the anastomotic unit, the test unit, the sensor unit, the mechanical drive unit, and the control unit (Fig. 1a and c; Fig. 2). Based on the perfusion bioreactor developed by Micheler et al. [31–33] the integrated system can be further categorized into two technologies: information technology and fluid power technology (Fig. 1a, b and d). The key components of the integrated system in this model include a human machine interface (HMI) (Fig. 3), a controller, actuators, sensors, a fluid system, and a sample

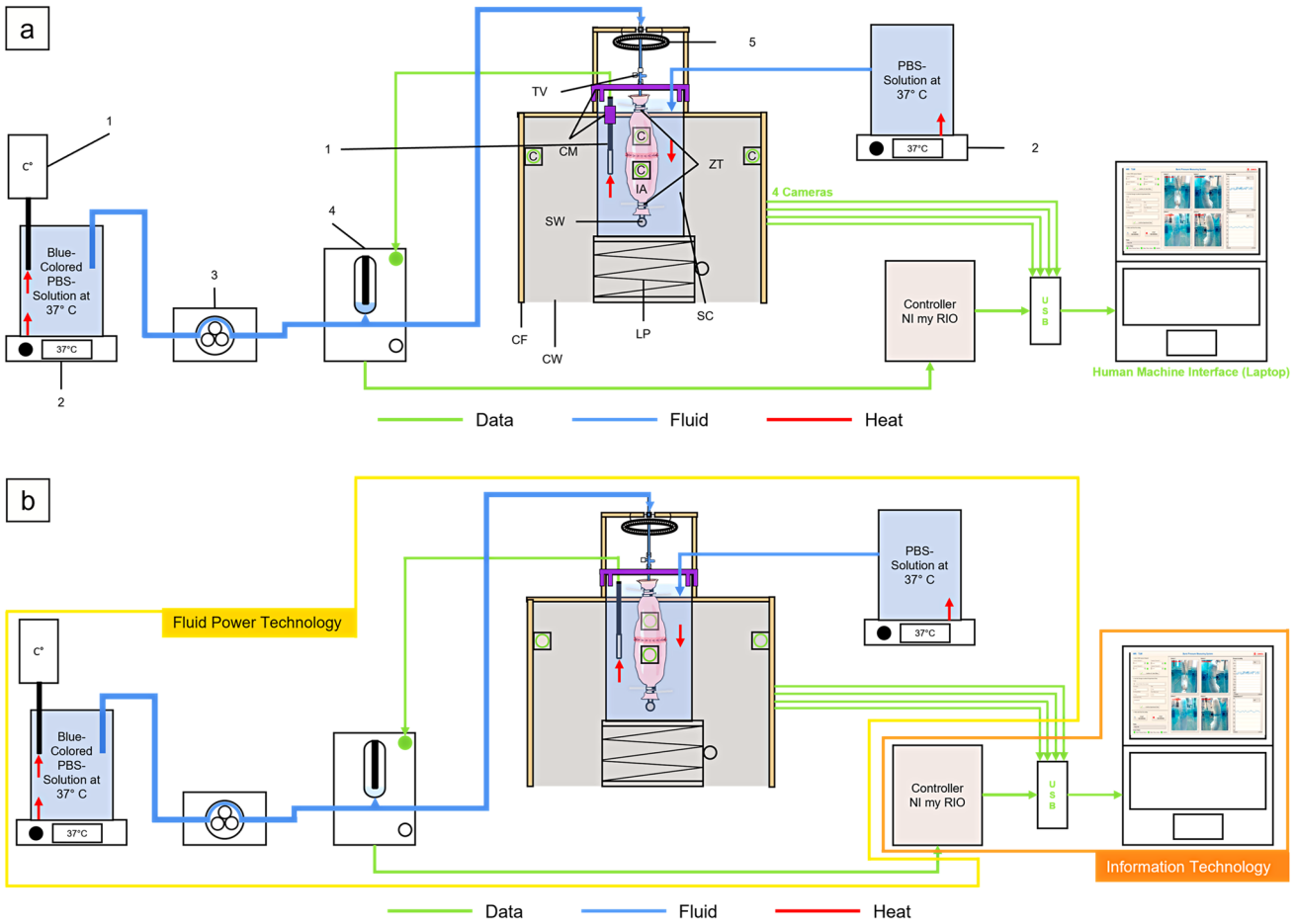

Fig. 1 Schematic representation of innovative *ex-vivo* model for evaluation of stability and pressure resistance of gastrointestinal anastomoses. (**a**) Schematic representation of the experimental setup illustrating the key components in the test configuration. (**b**) Schematic representation of the experimental setup categorized into two technologies: information technology and fluid power technology. (**c**) Schematic representation of the main units of the experimental setup: sensor unit; mechanical drive unit; test unit; anastomotic unit; control unit. (**d**) Modified perfusion bioreactor. Process description of the modified perfusion bioreactor, encompassing both information technology and fluid power technology. C = Camera; CF = Custom-made aluminum square shaped frame; CM = Custom-made 3D-printed stabilization brackets; CW = Custom-made plastic walls with cut-outs; IA = Intestinal anastomosis; LP = Laboratory lifting platform; SC = Sample chamber; SW = Stainless steel screw; TV = Three-way-valve; ZT = Zip ties; 1 = Temperature sensor; 2 = Heater; 3 = Peristaltic pump; 4 = Pressure sensor; 5 = LED Ring light. [31–33] (Modified from Micheler 2018a and Micheler, Geck, Charitou et al., Curr. Dir. Biomed. Eng 2021)

chamber. (Fig. 1a, b and d; Fig. 2; Supplementary Fig. 1; Supplementary Fig. 2) The two technologies and main components of the *ex-vivo* system are detailed in Supplementary Table 2.

Flow rate models

Two flow rate models were employed to simulate variations in fluid flow rates in the small intestine under different physiological conditions. Studies have shown that the fluid flow rate in the proximal small intestine is approximately 2.5 mL/minute (min) in fasting conditions [34, 35] and 20 mL/min after meals [36–40]. While the resting intraluminal pressure in the small intestine varies among the literature (6–13 mm of mercury (mmHg) [41–43] up to 20–30 mmHg during various peristaltic activities [44]), a sudden increase in intraabdominal and therefore intraluminal pressure can occur with activities, such as during Valsalva maneuvers (up to 40 mmHg), coughing (up to 100 mmHg), or jumping (up to 170 mmHg) [43, 45].

The low flow (LF) model with a fluid flow rate of 20 mL/min was utilized to simulate a physiological increase in intraluminal intestinal pressure under normal conditions (moderate increase in fluid influx, simulating the rise of intraabdominal pressure during regular activities).

The high flow (HF) model with a fluid flow rate of 200 mL/min was used to simulate a sudden increase in intraluminal intestinal pressure such as with coughing or jumping

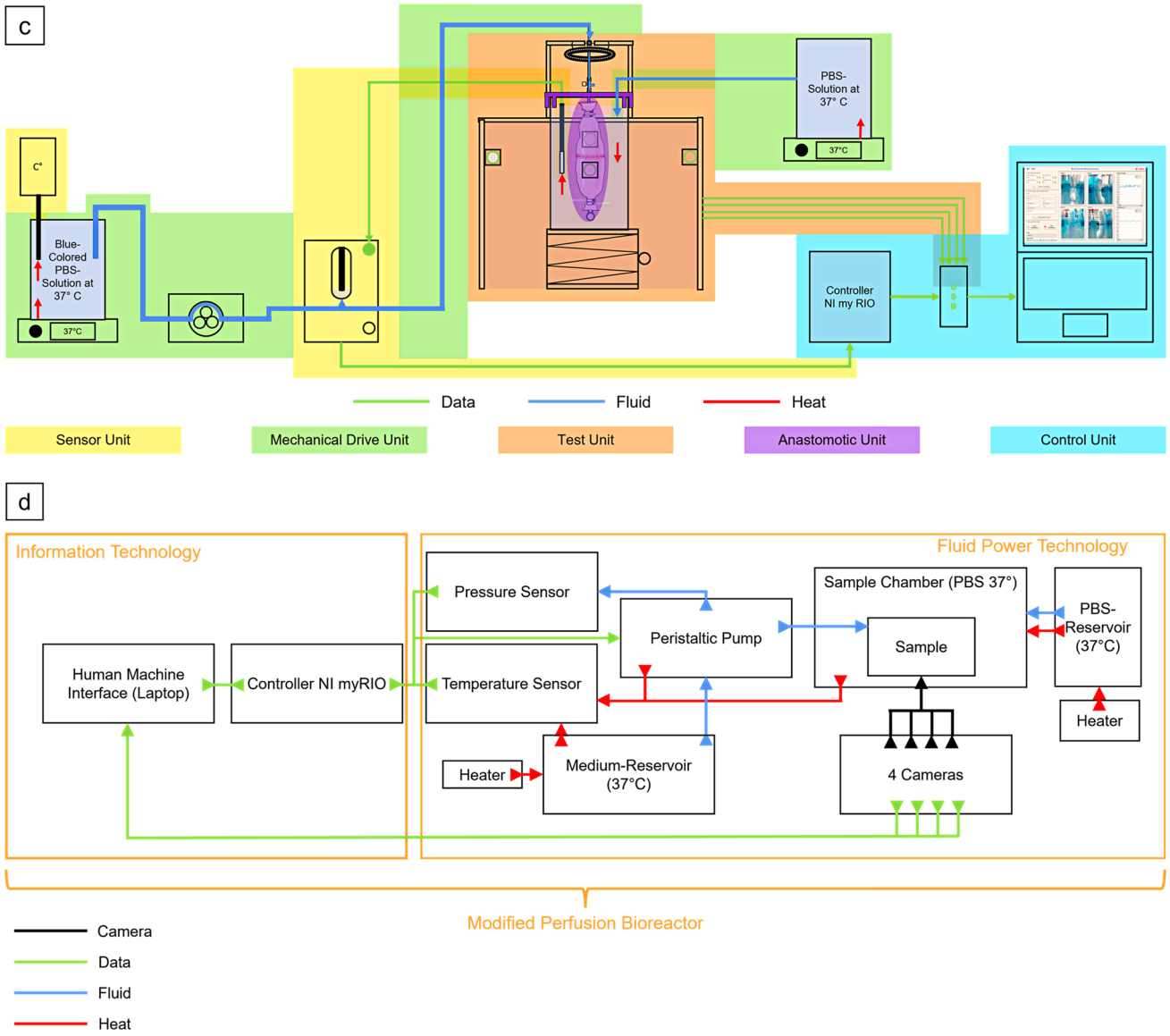

Fig. 1 (continued)

(substantial surge in fluid influx, simulating the abrupt elevation in intraabdominal pressure).

These two models aimed to replicate changes in the intraabdominal and therefore intraluminal pressure observed during different physiological states, providing a basis for studying the effects of pressure on anastomotic stability and pressure resistance.

Sample preparation and anastomotic techniques

Supplementary Fig. 3 illustrates the instruments and materials required to create the anastomotic unit.

The porcine small intestines were dissected into 20 cm (cm) long segments (Supplementary Fig. 4.a) and rehydrated at 37 °C before performing the intestinal anastomosis. Rehydration was performed with modification to the method described by Daristotle et al. [46] and involved submerging the segments in phosphate buffered saline solution preheated to 37 °C for five min. (Supplementary Fig. 4.a and 4.b).

For the feasibility trial, 32 handsewn sufficient end-to-end anastomoses were performed by one investigator (Kamacay Cira (K.C.)) on the porcine small intestine (cadaver of two pigs) in a random order, using either an interrupted single button suture (SBS) technique (n = 16) (Supplementary Fig. 5) or continuous suture (CS) technique (n = 16) (Supplementary Fig. 6). The suture material utilized for all anastomoses was 4–0 Polydioxanone. While only one surgeon conducted the anastomoses to minimize variability, another

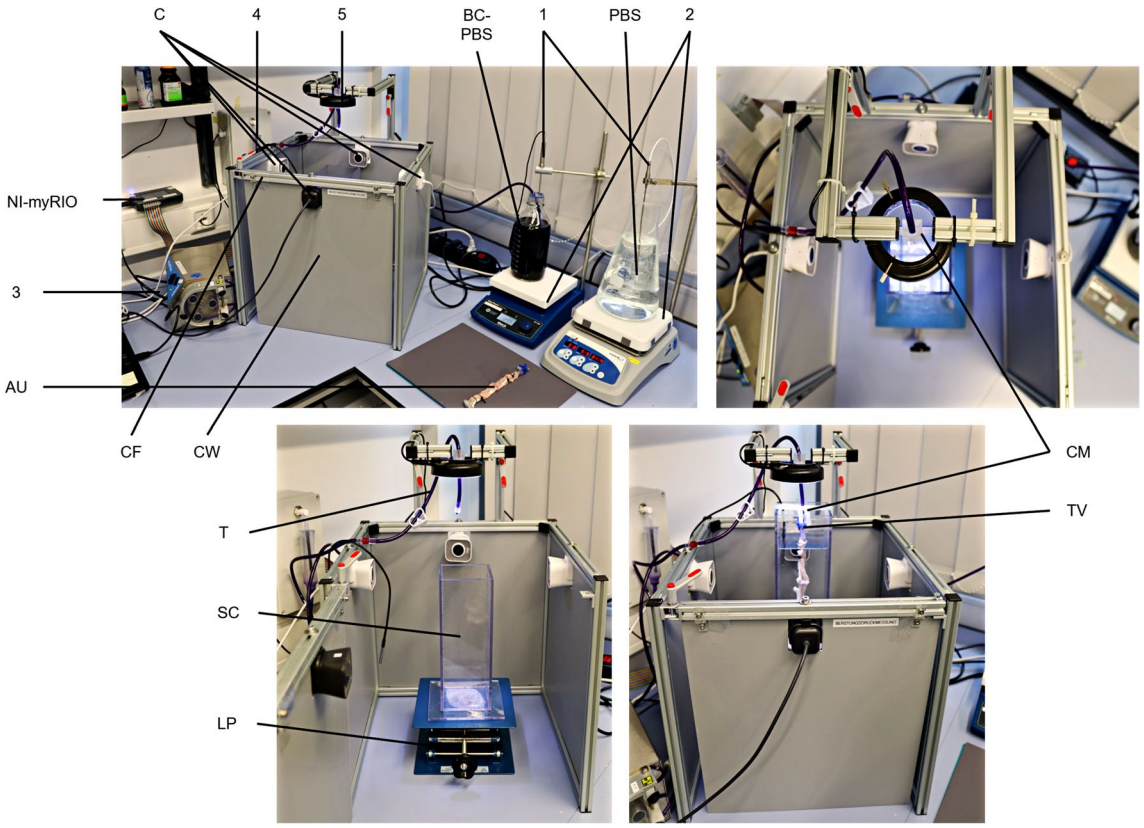

Fig. 2 Innovative *ex-vivo* model for evaluation of stability and pressure resistance of gastrointestinal anastomoses. BC-PBS = Blue-colored PBS-solution at 37 °C; C = Camera; CF = Custom-made aluminum square shaped frame; CM = Custom made 3D-printed stabilization brackets; CW = Custom-made plastic walls with cut-outs; LP = Laboratory lifting platform; NI-myRIO = NI-myRIO controller; PBS = PBS-solution at 37 °C; SC = Sample chamber; TV = Three-way-valve; T = Tube; ZT = Zip ties; 1 = Temperature sensor; 2 = Heater; 3 = Peristaltic pump; 4 = Pressure sensor; 5 = LED Ring light

Fig. 3 Human machine interface (computer) during an experiment. The figure displays the HMI on a computer used during the experiment. 1 = Camera activation: allows the user to activate the cameras for recording; 2 = Enter experimental data: enables inputting relevant experimental data; 3 = Start recording of the experiment: initiates the recording of the experiment; 4 = Stop recording of the experiment: halts the recording process; 5 = Video and sensor status: provides information on the status of videos and sensors; 6 = Four cameras capturing the anastomosis: shows the real-time footage from the four cameras capturing the anastomosis during the experiment; 7 = Pressure measurement: displays the intraluminal pressure

surgeon (Philipp-Alexander Neumann (P-A.N.), a senior surgeon) supervised the performance of the anastomoses to eliminate systematic technical errors. The anastomoses were further divided randomly by another investigator (Saskia Nicole Janett (S.N.J.)) into the following four experimental series:

a) *Experimental series 1 (SBS-LF)*: eight handsewn sufficient small intestinal SBS end-to-end anastomoses were created. (Supplementary Figure 5) These anastomoses were subsequently tested in the LF model;
b) *Experimental series 2 (SBS-HF)*: eight handsewn sufficient small intestinal SBS end-to-end anastomoses were created. (Supplementary Figure 5) These anastomoses were subsequently tested in the HF model;
c) *Experimental series 3 (CS-LF)*: eight handsewn sufficient small intestinal CS end-to-end anastomoses were created. (Supplementary Figure 6) These anastomoses were subsequently tested in the LF model;
d) *Experimental series 4 (CS-HF)*: eight handsewn sufficient small intestinal CS end-to-end anastomoses were created. (Supplementary Figure 6) These anastomoses were subsequently tested in the HF model.

Data analysis

Detailed data analysis is presented in Supplementary Table 3. Key parameters, including start pressure, LP, BP and various time intervals, were quantitatively studied to assess anastomotic performance (Fig. 4). These measurements prove insights into anastomotic integrity and endurance under different intraluminal pressures, simulating e.g. physiological and forceful expiratory activities. For more detailed information on the definition of different key parameters and a description of data acquisition procedures, please refer to Supplementary Table 4. Interrelated analyses were conducted on the outcomes of different experimental series to understand the temporal relationship between LP and BP, as well as the pressure and time differences associated with these events. More information about parameter definitions, data acquisition procedures, and their significance can be found in Supplementary Table 5.

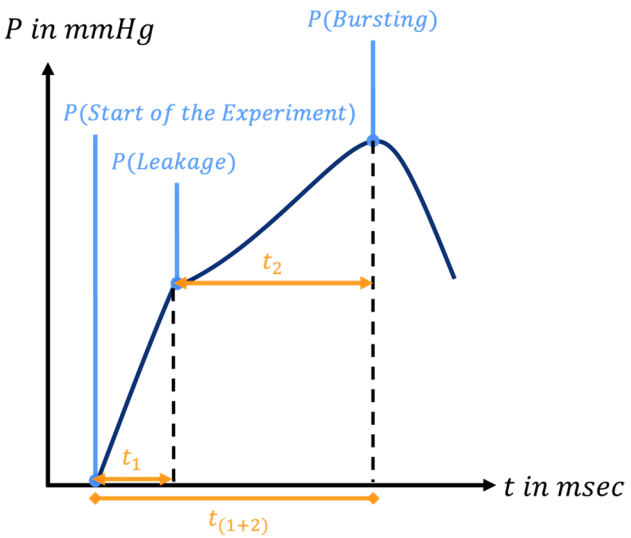

Fig. 4 Analysis of key parameters during the experimental process. This figure presents key parameters of the experimental process, including start pressure, LP, BP, and time intervals. mmHg = millimeters of mercury; msec = millisecond; P = Pressure; t = time; t_1 = Start to LP Time; t_2 = LP to BP; Time; $t_{(1+2)}$ = Start to BP Time

Leakage and bursting location analysis

In order to investigate the location of leakage and bursting of the porcine small intestinal anastomoses, images from all four cameras capturing different angles of the anastomosis were correlated with the corresponding measured pressures for each experimental trial. The anastomosis was divided into eleven equal sections, numbered from -5 to 5, with 0 (or M0) representing the precise location of mesenteric attachment to the intestine (Figs. 5 and 6).

To simplify data evaluation and presentation, these circular sections were transformed into a linear grid, with 0 positioned at the center, -5 to the far left, and 5 to the far right. The grid was further divided into two zones: the mesenteric zone (between -1 and + 1) and the peripheral zone (ranging from -2 to -5 and + 2 to + 5), labeled as zones M1 and P (P2 – P5) respectively (Fig. 6).

After marking the locations of leakage and bursting based on the corresponding images of each anastomosis, the number of occurrences per zone was assessed for each experimental trial. Comparisons were made to explore the occurrence of leakage and bursting between the mesenteric and peripheral zones within each experimental series and across different experimental groups. Additionally, a general comparison was performed to determine if leakage and bursting tended to manifest more frequently in either the mesenteric or peripheral zone across all experimental groups (Fig. 6).

Statistical analysis

Outcomes with a p-value of ≤ 0.05 in this study are considered as significant. Microsoft Excel and GraphPad Prism were used for statistical analyses. Descriptive statistics were computed, providing various parameters like mean, standard error (*SEM*), median, standard deviation (*SD*), sample variance, kurtosis, skewness, range (minimum, maximum), sum, count, and a 95% confidence level with upper and lower limits. The upper and lower confidence intervals (*CI*) were calculated for comparisons within experimental series. To compare the results of the descriptive statistical analysis

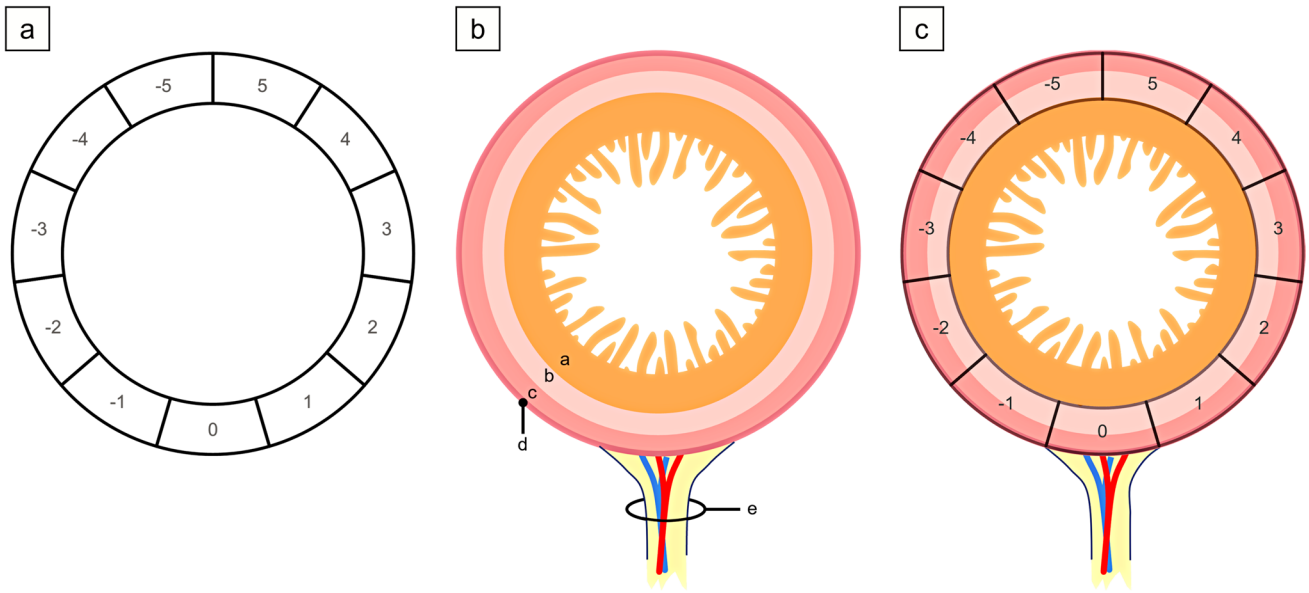

Fig. 5 Location analysis of anastomotic leakage and bursting in small intestinal anastomoses. (a) The circular section model depicts the anastomoses partitioned into eleven equidistant sections, designated by numbers ranging from -5 to 5. The reference point, 0 (or M0), precisely indicates the location of the mesenteric attachment to the intestine. (b) Schematic cross-section of the small intestine. (c) The composite presentation of (a) and (b) provides insights into the spatial distribution of the eleven equidistant sections. a = Tunica mucosa; b = Tunica submucosa; c = Tunica muscularis; d = Tunica serosa; e = Mesentery

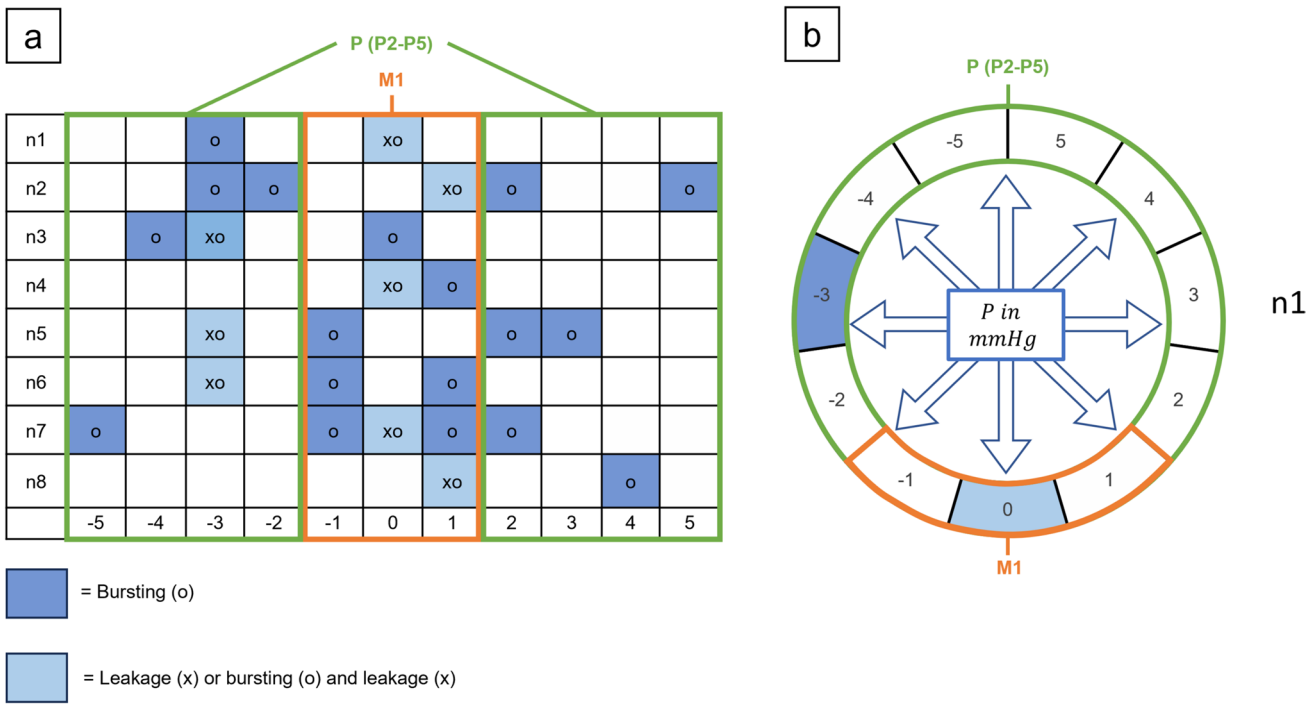

Fig. 6 Location analysis: Spatial distribution of anastomotic leakage and bursting in small intestinal anastomoses. (a) To simplify data evaluation and presentation, the circular sections were transformed into a linear grid, with 0 at the center, -5 to the far left, and 5 to the far right. The grid was further divided into two zones: the mesenteric zone (between -1 and + 1, labeled as zone M1) and the peripheral zone (ranging from -2 to -5 and + 2 to + 5, labeled as zone P (P2-P5)). Leakage points are marked with "x" and bursting points with "o". (b) The circular section model represents n1 on the grid

among the experimental series, the Mann–Whitney U test [47, 48], a non-parametric test suitable for comparing two independent groups, especially when data isn't normally distributed or sample sizes are small, was employed. The Fisher's exact test [49], a statistical tool suitable for analyzing categorical data with small sample sizes, was employed to analyze and compare the incidence of leakage and bursting within and between areas of the anastomosis – specifically, the mesenteric zone and peripheral zone – across each of the four experimental groups.

The Odds ratio (*OR)* was used in this study to assess the association and quantify the strength of relationships between different aspects of anastomotic performance, with a particular focus on leakage and bursting rates at specific locations within the anastomosis.

Results

A total of 32 handsewn small intestinal end-to-end anastomoses were performed. Half of these anastomoses were constructed using the SBS technique (Supplementary Fig. 5), while the other half utilized the CS technique (Supplementary Fig. 6). Within each suture technique group, half of the anastomoses were tested in the LF model, while the remaining half were tested in the HF. Figure 7 illustrates the pressure–time profiles of the individual groups, whereby Fig. 7a presents the SBS-LF group, Fig. 7b the SBS-HF group, Fig. 7c the CS-LF group, and Fig. 7d the CS-HF group. Descriptive statistical analysis results for LP, BP, and time intervals can be found in Supplementary Tables 6–13. Interrelated analyses from experimental outcomes are presented in Supplementary Tables 10–13 and Supplementary Figs. 7–9.

Quantitative analysis of anastomotic performance and time intervals: comparison within the experimental series

Leakage pressure analysis

For SBS-anastomoses, the HF model showed a statistically significantly higher LP compared to the LF model ($p = 0.0281$; exact 95.01% *CI* for the difference ranging from

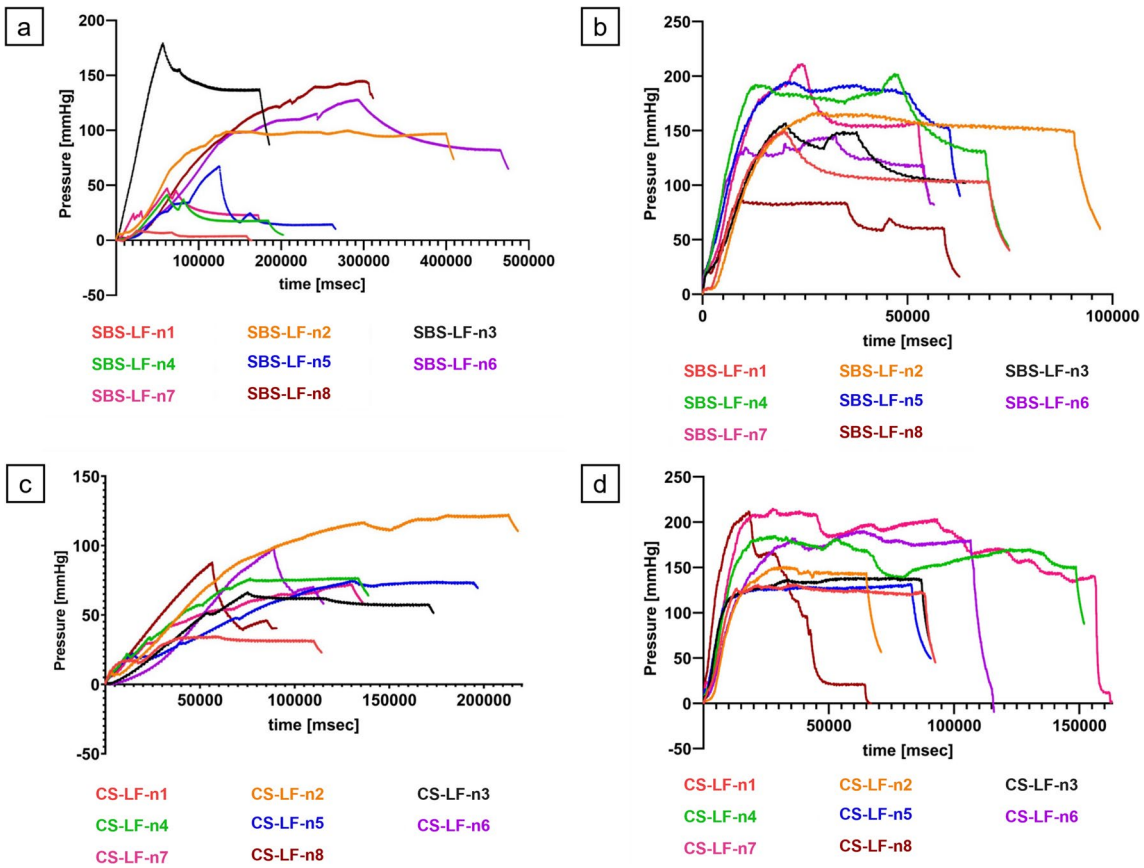

Fig. 7 Pressure–time profiles of all anastomoses. a. SBS-LF anastomoses. b. SBS-HF anastomoses. c. CS-LF anastomoses. d. CS-HF anastomoses. mmHg = Millimeters of mercury; msec = Milliseconds

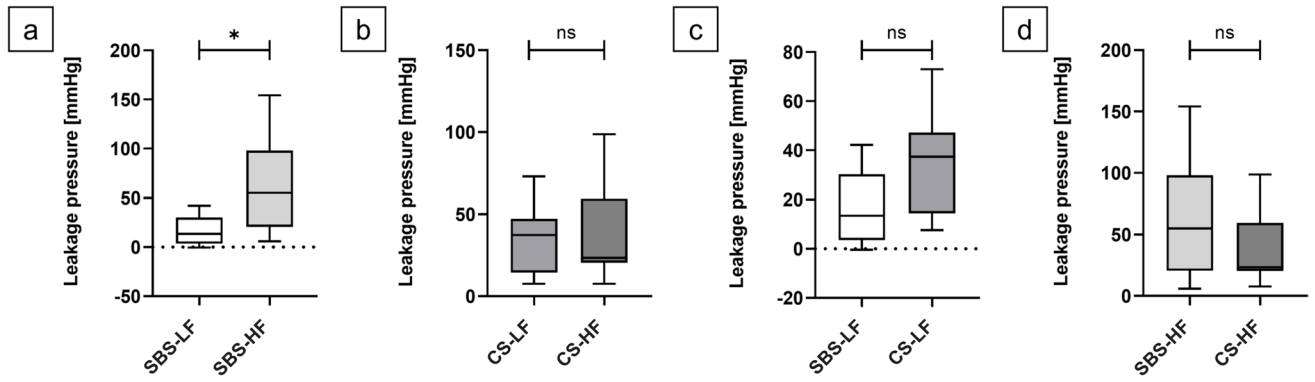

Fig. 8 Leakage pressure (LP) comparison among experimental series. Box plots of anastomotic LP values (mmHg) comparing SBS-LF with SBS-HF anastomoses, CS-LF with CS-HF anastomoses, SBS-LF with CS-LF anastomoses and SBS-HF with CS-HF anastomoses. (**a**) SBS-HF anastomoses had a statistically significantly higher LP compared to SBS-LF anastomoses ($p=0.0281$). (**b**) No significant difference in LP was seen between CS-LF and CS-HF ($p=0.9043$); (**c**) SBS-LF and CS-LF ($p=0.0830$) and (**d**) SBS-HF and CS-HF ($p=0.3823$) anastomoses. Significance was assessed using Mann–Whitney U tests

4.200 to 81.50). (Fig. 8a) However, no statistically significant differences for LP were observed between the two flow models for CS-anastomoses ($p=0.9043$; exact 95.01% *CI* of difference -23.8 to 24.80) (Fig. 8b). Additionally, there were no significant differences in LP between the two suture techniques, regardless of the flow model employed (SBS-LF vs. CS-LF anastomoses: $p=0.0830$; exact 95.01% *CI* of difference -1.300 to 39.00 (Fig. 8c); SBS-HF and CS-HF anastomoses: $p=0.3823$; exact 95.01% *CI* of difference -73.50 to 15.80 (Fig. 8d)).

Bursting pressure analysis

For SBS-anastomoses ($p=0.0115$; exact 95.01% *CI* for the difference ranging from 18.60 to 136.3) (Fig. 9a) and CS-anastomoses ($p=0.0002$; exact 95.01% *CI* of difference of 56.60 to 124.0) (Fig. 9b), the HF model showed a statistically significant higher BP compared to the LF model.

However, no statistically significant differences for BP was observed between the two suture techniques, regardless of the flow model employed (SBS-LF vs. CS-LF anastomoses: $p=0.7984$; exact 95.01% *CI* of difference -65.40 to 40.40 (Fig. 9c); SBS-HF and CS-HF anastomoses: $p>0.9999$; exact 95.01% *CI* of difference -34.90 to 45.80 (Fig. 9d).

Time interval analysis

Time interval from start to leakage For SBS-anastomoses ($p=0.0011$; exact 95.01% *CI* for the difference ranging from -35,014 to -6537) (Supplementary Fig. 10.a) and CS-anastomoses ($p=0.0006$; exact 95.01% *CI* of difference

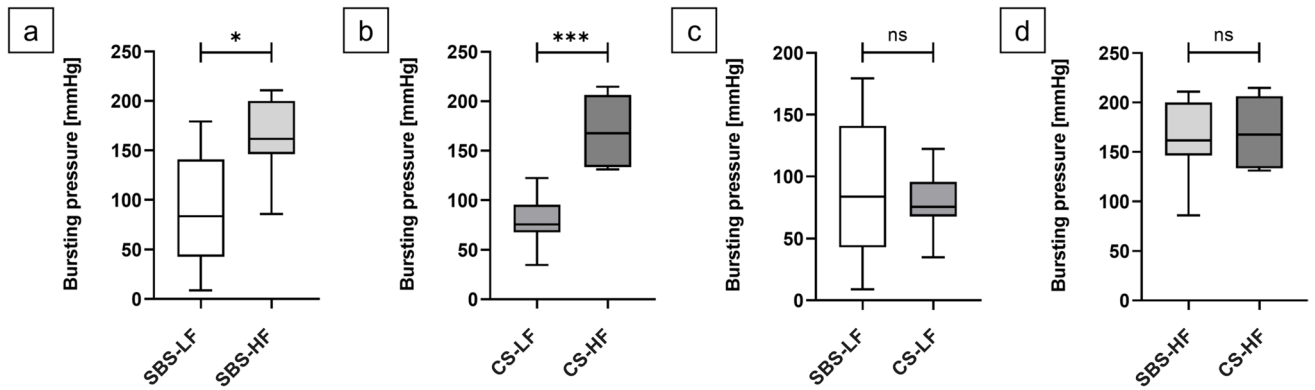

Fig. 9 Bursting pressure (BP) comparison among experimental series. Box plots of anastomotic BP values (mmHg) comparing SBS-LF with SBS-HF anastomoses, CS-LF with CS-HF anastomoses, SBS-LF with CS-LF anastomoses and SBS-HF with CS-HF anastomoses. (**a**) SBS-HF anastomoses had a statistically significantly higher BP compared to SBS-LF anastomoses ($p=0.0115$). (**b**) CS-HF anastomoses had a statistically significantly higher BP compared to CS-LF anastomoses ($p=0.0002$). No significant difference in BP was seen between (**c**) SBS-LF and CS-LF ($p=0.7984$) and (**d**) SBS-HF and CS-HF ($p>0.9999$) anastomoses. Significance was assessed using Mann–Whitney U tests

of -52,502 to -12,748) (Supplementary Fig. 10.b), LP was reached significantly faster in the HF model compared to the LF model. However, no statistically significant differences in time from start to LP was observed between the two suture techniques, regardless of the flow model employed (SBS-LF vs. CS-LF anastomoses: $p = 0.6454$; exact 95.01% *CI* of difference -11,620 to 27,900 (Supplementary Fig. 10.c); SBS-HF and CS-HF anastomoses: $p = 0.7984$; exact 95.01% *CI* of difference from -5519 to 1603 (Supplementary Fig. 10.d)).

Time interval from start to bursting For SBS-anastomoses ($p = 0.0011$; exact 95.01% *CI* for the difference ranging from -251,503 to -29,704) (Supplementary Fig. 11.a) and CS-anastomoses ($p = 0.0070$ exact 95.01% *CI* of difference of -102,910 to -24,341) (Supplementary Fig. 11.b), BP was reached significantly faster in the HF model compared to the LF model. However, no statistically significant differences in time from start to BP was observed between the two suture techniques, regardless of the flow model employed (SBS-LF vs. CS-LF anastomoses: $p = 0.7984$; exact 95.01% *CI* of difference -148,167 to 69,700 (Supplementary Fig. 11.c); SBS-HF and CS-HF anastomoses: $p = 0.0830$; exact 95.01% *CI* of difference from -299.0 to 45,694 (Supplementary Fig. 11.d)).

Time interval from leakage to bursting BP was reached significantly faster after LP for SBS-anastomoses in the HF model compared to the LF model ($p = 0.0070$; exact 95.01% *CI* for the difference ranging from -214,300 to -14,104) (Supplementary Fig. 12.a) and compared to CS-anastomoses in the HF model ($p = 0.0379$ exact 95.01% *CI* of difference of 141.0 to 50,402) (Supplementary Fig. 12.b). No significant differences in time from LP to BP were observed between the two flow models for CS-anastomoses ($p = 0.0650$, exact 95.01% *CI* of difference ranging from -76,674 to 3710) (Supplementary Fig. 12.c). Furthermore, no significant difference was observed between the LF model of both suture techniques ($p = 0.9591$; exact 95.01% *CI* of difference from -127,995 to 54,551 (Supplementary Fig. 12.d)).

Descriptive analysis of leakage and bursting location

Leakage and bursting location analysis

For the SBS-LF and SBS-HF groups respectively, a total of eight (LP), 18 and 16 (BP) anastomotic locations with LP in the mesenteric zone were observed, while 16 (LP), six and eight (BP) anastomotic locations in the mesenteric zone did not exhibit leakage. In the peripheral zone, seven and two (LP), and twelve and 13 (BP) anastomotic locations displayed leakage, while 57 and 62 (LP), and 52 and 51 (BP) anastomotic locations remained free from leakage. For the CS-LF and CS-HF groups respectively, seven (LP), 20 and 22 (BP) and anastomotic locations exhibited leakage in the mesenteric zone, while 17 (LP), four and two (BP) anastomotic locations in the mesenteric zone did not show leakage. In the peripheral zone, two (LP), 20 and 22 (BP) anastomotic locations displayed leakage, while 62 (LP), 44 and 42 (BP) anastomotic locations remained free from leakage (Fig. 10).

Association between leakage and bursting locations

Among all cases of leakage observed in the study, with the exception of one, it was found that the anastomoses at the leakage location side also exhibited bursting. This consistent pattern suggests a strong association between leakage occurrence and the risk of bursting at the same location within the anastomosis.

Leakage and bursting location analysis: comparison within and between the experimental series

No differences were observed in AL rates of areas within the mesenteric zone (Supplementary Fig. 13) and within the peripheral zone (Supplementary Fig. 14) among compared experimental series. Similarly, no differences were observed in BP rates of areas within the mesenteric zone (Supplementary Fig. 15) and within the peripheral zone (Supplementary Fig. 16) among compared experimental series.

Differences in anastomotic leakage rates between areas of the mesenteric and the peripheral zone

The incidence of leakage in the SBS -LF anastomoses was significantly higher in the mesenteric zone compared to the peripheral zone ($p = 0.0230$; *OR*, 4.071). Similarly, SBS-HF anastomoses ($p = 0.0003$; *OR*, 15.50); CS-LF anastomoses ($p = 0.0013$; *OR*, 12.76), and CS-HF anastomoses ($p = 0.0013$; *OR*, 12.76) exhibited significantly higher incidences of leakage at the mesenteric zone compared to the peripheral zone (Fig. 11).

Therefore, irrespective of the anastomotic technique or flow rate model utilized, anastomoses exhibited a significantly higher incidence of leakage at the mesenteric entry side compared to other sections of the anastomosis.

Differences in anastomotic bursting rates between areas of the mesenteric and the peripheral zone

Significantly higher incidences of bursting in the SBS-LF anastomoses were observed in the mesenteric zone compared to the peripheral zone ($p < 0.0001$; *OR*, 13.00). Similarly, SBS-HF anastomoses zone ($p < 0.0001$; *OR*, 7.846), CS-LF anastomoses ($p < 0.0001$; *OR*, 11.00), and CS-HF anastomoses ($p < 0.0001$; *OR*, 21.00) exhibited a

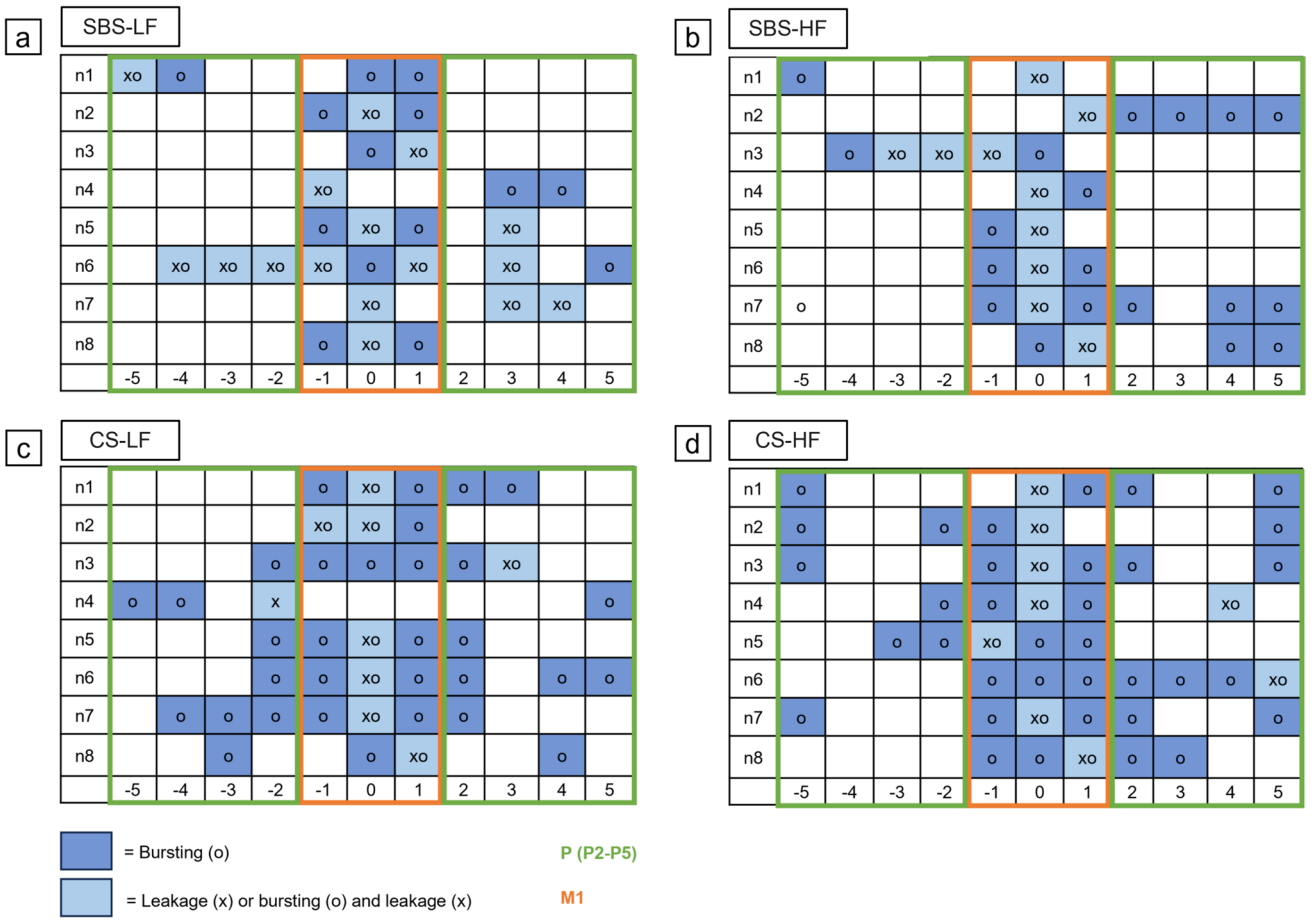

Fig. 10 Location analysis: Spatial distribution of anastomotic leakage and bursting in the experimental series. The figure illustrates a linear grid, distinguishing between two zones: the mesenteric zone (between -1 and + 1, labeled as zone M1) and the peripheral zone (ranging from -2 to -5 and + 2 to + 5, labeled as zone P (P2-P5)). Leakage points are marked with "x" and bursting points with "o". (a) SBS-LF anastomoses. (b) SBS-HF anastomoses. (c) CS-LF anastomoses. (d) CS-HF anastomoses

significantly higher incidence of bursting at the mesenteric zone compared to the peripheral (Fig. 12).

Therefore, irrespective of the experimental series or anastomotic technique used, anastomoses exhibited a significantly higher incidence of bursting at the mesenteric entry side compared to other sections of the anastomosis.

Discussion

The herein used *ex-vivo* model allows for comparable, reproducible and user-independent investigation of anastomotic biomechanics under controlled conditions. It is important to note that the goal was not to precisely replicate *in-vivo* intestinal stress but rather to induce stress on the tissue wall in a manner reflective of observed human stress situations. This approach allows analysis of biomechanical behavior, specifically stretching and stiffness, and offers the advantage of identifying technical weak points of gastrointestinal anastomoses. Surgeons can utilize this information to improve their techniques and minimize technical-associated AL.

Results from the experiment unveiled significant differences in LP, BP and time intervals, influenced by the chosen flow models (Figs. 8 and 9; Supplementary Figs. 7–12). These variances likely stem from time-dependent stress–strain reactions inherent in the viscoelastic properties of biological tissues. Rapid influx of fluid leads to an abrupt pressure surge due to immediate elastic response, but viscous behavior causes continuous stretching over time until the tissue eventually bursts. In contrast, under slow loading conditions, the viscous tissue element has more time to react, resulting in a gradual stress–strain response. When stress is removed, faster relaxation occurs. Consequently, with a lower rate of intraluminal fluid influx, the tissue experiences a gradual pressure increase, matching its viscous response to the pace of deformation. This leads to the attainment of a lower final pressure before tissue bursting

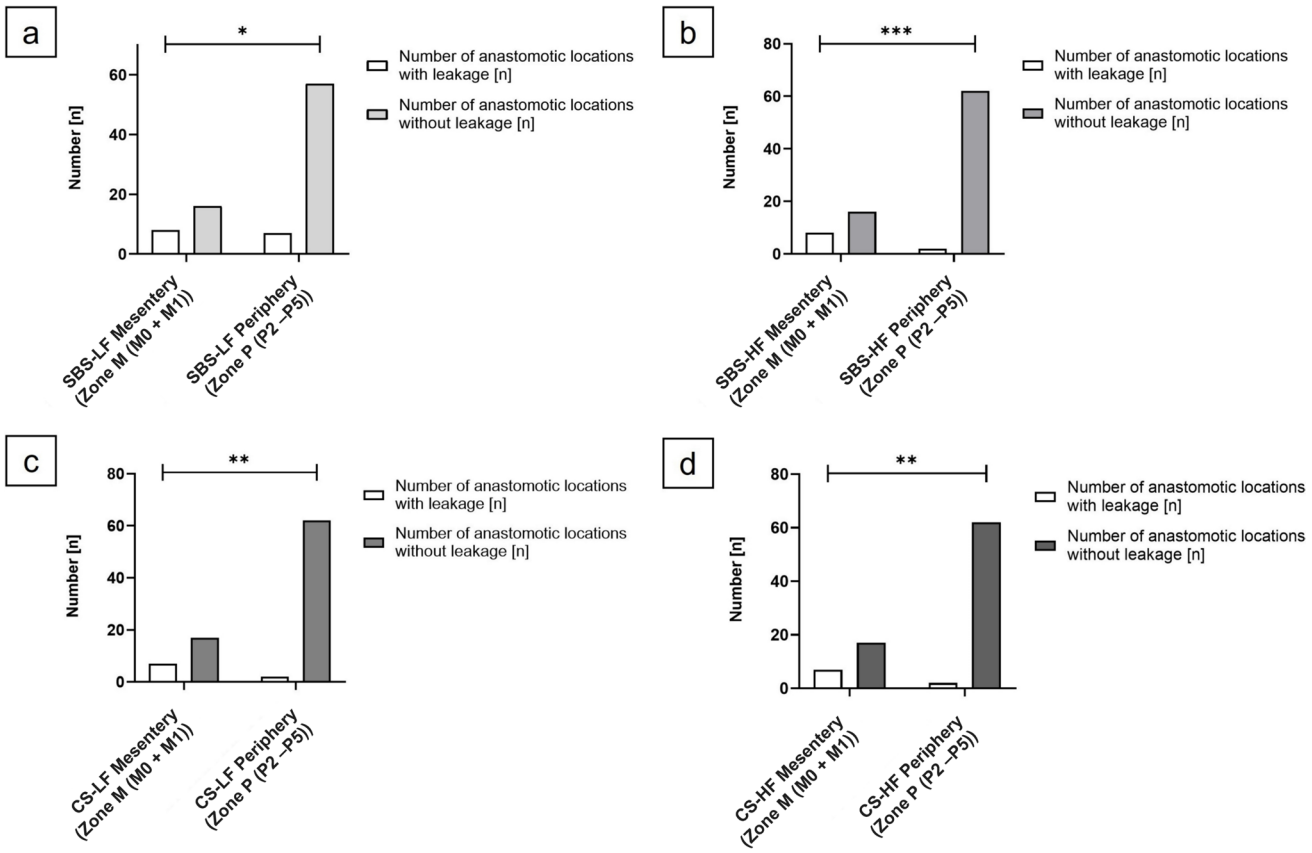

Fig. 11 Differences in anastomotic leakage rates between the areas of the mesenteric and the peripheral zone. (a) SBS-LF anastomoses ($p=0.0230$), (b) SBS-HF anastomoses ($p=0.0003$), (c) CS-LF anastomoses ($p=0.0013$), and (d) CS-HF anastomoses ($p=0.0013$) exhibited a statistically significantly higher incidence of leakage at the mesenteric zone compared to the peripheral zone. Significance was assessed using Fisher's exact test. *$p<0.05$; ** $p<0.01$; *** $p=<0.001$

[24–27, 50–52]. Importantly, the choice of suture technique appeared to have no considerable impact on either LP or BP, indicating minimal influence on the stability and pressure resistance of the end-to-end anastomoses. The fact that these results can be detected by the *ex-vivo* model further strengthens its relevance in investigating anastomotic biomechanics.

One of the central findings emphasize the association between leakage and bursting and the specific location within the anastomosis, particularly the insertion site of the mesentery. This supports the assumption that the insertion site of the mesentery represents a vulnerable point where AL can develop. The insertion site of the mesentery serves as a potential weak spot due to its role as a transition area between the mobile and fixed parts of the intestine. Here, the mesentery, responsible for blood supply and nerve innervation, attaches to the intestinal wall, creating a point of stress concentration that increases the susceptibility to mechanical failure or disruption [53]. Anastomoses performed at the insertion site of the mesentery during surgical procedures compound the risk as they weaken the tissue and elevate the likelihood of complications such as AL. However, factors such as suture quality, tissue healing response, and mechanical stress also contribute to the risk of leakage in this specific anatomical location [54–58].

Given the clinical significance of anastomotic complications, careful evaluation and management of the insertion site of the mesentery during surgical procedures are crucial. Surgeons should exercise caution and employ appropriate techniques to ensure secure and reliable anastomoses at this critical location. Exploring advancements in surgical techniques, including reinforcement methods or innovative approaches to strengthen the anastomotic site, is essential to mitigate the risk of complications and improve patient outcomes. By gaining a better understanding of potential weak spots in anastomoses, such as the insertion site of the mesentery, surgeons can make informed decisions and implement strategies to minimize the occurrence of AL. Collaborative efforts between surgeons and researchers, along with future research endeavors, are warranted to refine surgical techniques, develop novel interventions, and enhance patient safety in the context of anastomotic procedures.

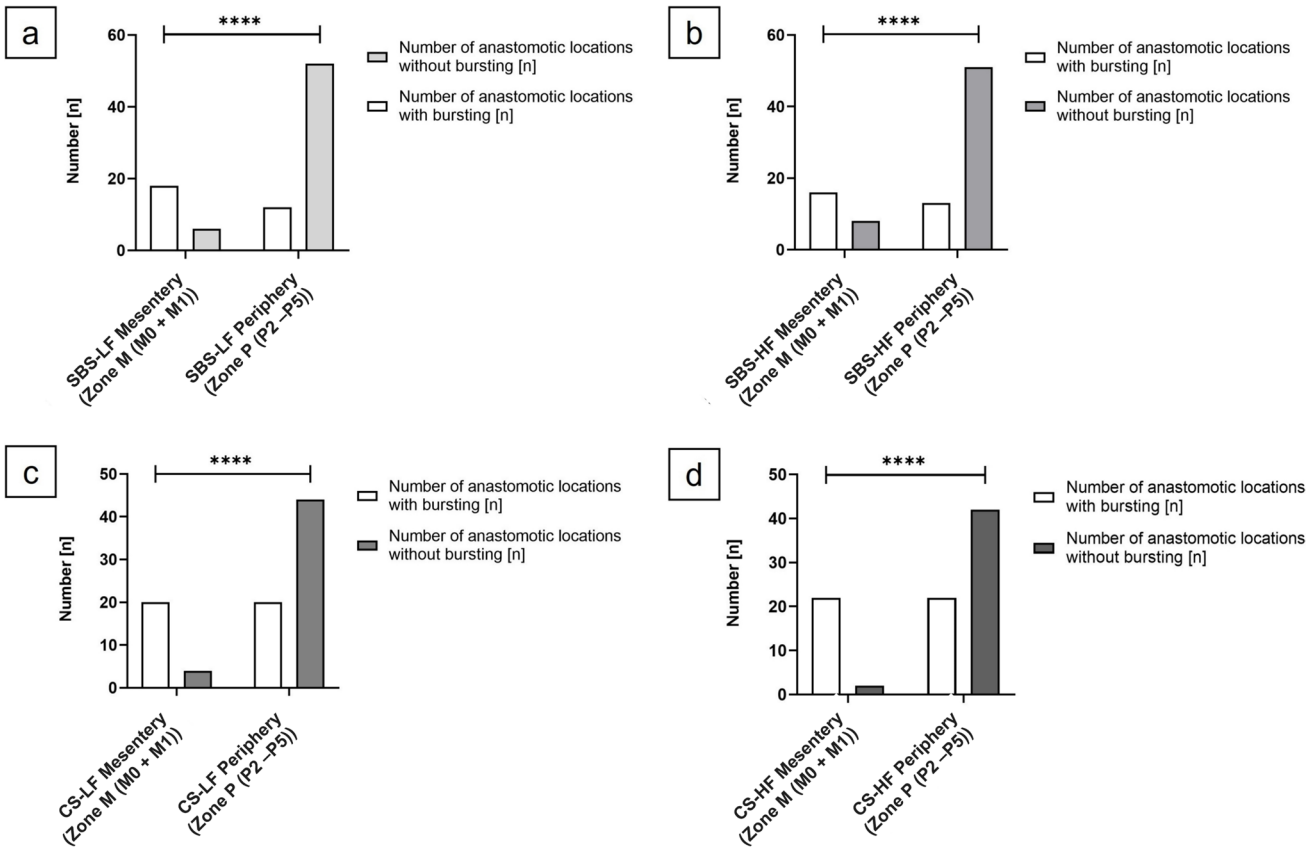

Fig. 12 Differences in anastomotic bursting rates between the areas of the mesenteric and the peripheral zone. (a) SBS-LF anastomoses ($p < 0.0001$), (b) SBS-HF anastomoses ($p < 0.0001$), (c) CS-LF anastomoses ($p < 0.0001$), and (d) CS-HF anastomoses ($p < 0.0001$) exhibited a statistically significantly higher incidence of bursting at the mesenteric zone compared to the peripheral zone. Significance was assessed using Fisher's exact test. *$p < 0.05$; ** $p < 0.01$; *** $p = < 0.001$; **** $p < 0.0001$

The inherent limitations of the model align with challenges commonly observed in *ex-vivo* models, as they face difficulties in reproducing the complex physiological conditions present in *in-vivo* settings. Variables such as blood flow, tissue perfusion, and dynamic physiological forces are inadequately simulated. The *ex-vivo* model was intentionally designed to focus on investigating the biomechanical properties of various anastomotic techniques and the effects of different pressure conditions. While acknowledging the inability to fully replicate *in-vivo* complexity, deliberate simplifications and controlled conditions allow for isolating and scrutinizing specific biomechanical aspects. This focus aligns with the rationale that a comprehensive understanding of these mechanical factors is crucial for refining surgical techniques and optimizing outcomes. While this model may not capture the full spectrum of biological complexities, its intentional design provides a valuable niche for investigating biomechanical dimensions critical to anastomotic procedures. Further research can build upon these findings to enhance our understanding of broader biological healing processes in gastrointestinal surgeries.

Another limitation important to note is the variability among the samples. The test setup aimed to objectively quantify *ex-vivo* AL and bursting detection by standardizing parameters essential biomechanical measurements, such as temperature, pH or pressure differences. It is crucial to recognize that the experimental model is intentionally crafted to accommodate inherent variations, especially within an *ex-vivo* context where tissue-related factors and surgical techniques introduce an anticipated level of variability. Despite this acknowledged variation, the model has demonstrated its ability to discern significant differences, such as distinguishing between LF and HF models. Furthermore, the potential impact of sample size on variation is recognized and increasing it could additionally alleviate this concern. These considerations underscore the robustness of the model in capturing and distinguishing pertinent biomechanical properties.

Finally, a standardization and automation of the *ex-vivo* model for suture evaluation represent a commendable initiative with the potential to pave the way for future regulatory frameworks governing the authorization of new stapling systems. By establishing a uniform and

automated testing protocol, the reliability and reproducibility of suture evaluations can be significantly enhanced. This not only ensures consistency in assessing the performance of various stapling systems but also provides a basis for developing robust regulatory guidelines. Such guidelines, rooted in standardized testing methodologies, can contribute to the systematic evaluation of new stapling systems, fostering innovation, safety, and efficacy in surgical practices. The integration of these advancements into regulatory frameworks may prove instrumental in shaping the landscape of stapling system authorization, promoting advancements in surgical technology, and enhancing patient care.

In conclusion, this study provides a valuable contribution to the understanding of gastrointestinal anastomoses' biomechanics through an application of an operator-independent *ex-vivo* model generating comparable and reproducible results. The experimental results revealed significant differences in anastomoses' LP, BP, and time intervals based on flow models, attributed to their inherent biomechanical properties as biologic tissue. The choice of suture technique did not significantly affect LP and BP, suggesting that it may not have a substantial impact on anastomotic stability and pressure resistance. Most interestingly, the observed higher leakage and bursting rates at the insertion site of the mesentery suggest that this site displays specific biomechanical properties, rendering it a potential weak spot for anastomosis, and making it more prone to AL development. Surgical techniques and devices should adapt to this potential weak spot to minimize the risk of mechanically induced AL.

Supplementary Information The online version contains supplementary material available at https://doi.org/10.1007/s00423-024-03318-8.

Acknowledgements The authors would like to acknowledge the Center of Preclinical Research affiliated with the Klinikum rechts der Isar of the Technical University of Munich for their support in providing animal material obtained from animals sacrificed for other purposes.

Author contributions KC, AO; RB and P-AN contributed to the conception and design of the study. KC and SNJ were involved in data collection. KC perfomed quantitative and qualitative analyses. CM, AO, RB engineered device. P-AN assessed the accuracy of the data. KC organized the database. KC performed the statistical analysis. KC created figures and tables. KC drafted the manuscript. SNJ, CM, SH, AO; RB, HF and P-AN, revised the manuscript for important intellectual contents. All authors contributed to manuscript revision, read, and approved the submitted version. P-AN and RB were responsible for funding.

Funding Open Access funding enabled and organized by Projekt DEAL. This study was supported by the Bavarian Research Foundation (grant number: AZ-1508–21). Open Access funding was enabled and organized by the german Project DEAL.

Data availability The authors confirm that the data supporting the findings of this study are available within the article and its supplementary materials.

Declarations

Competing interests The authors declare no competing interests.

References

1. Akasu T, Takawa M, Yamamoto S, Yamaguchi T, Fujita S, Moriya Y (2010) Risk factors for anastomotic leakage following intersphincteric resection for very low rectal adenocarcinoma, (in eng). J Gastrointest Surg 14(1):104–111. https://doi.org/10.1007/s11605-009-1067-4
2. Bader FG, Schröder M, Kujath P, Muhl E, Bruch HP, Eckmann C (2009) Diffuse postoperative peritonitis – value of diagnostic parameters and impact of early indication for relaparotomy, (in eng). Eur J Med Res 14(11):491–496. https://doi.org/10.1186/2047-783x-14-11-491
3. Doeksen A, Tanis PJ, Vrouenraets BC, Gooszen JA, van Lanschot JJ, van Tets WF (2007) Outcome of rectal cancer surgery after the introduction of preoperative radiotherapy in a low-volume hospital, (in eng). J Gastrointest Cancer 38(2–4):63–70. https://doi.org/10.1007/s12029-008-9018-y
4. Hagens ERC, Reijntjes MA, Anderegg MCJ, Eshuis WJ, van Berge Henegouwen MI, Gisbertz SS (2021) Risk factors and consequences of anastomotic leakage after esophagectomy for cancer. Ann Thoracic Surg 112(1):255–263. https://doi.org/10.1016/j.athoracsur.2020.08.022
5. Kang CY et al (2013) Risk factors for anastomotic leakage after anterior resection for rectal cancer, (in eng). JAMA Surg 148(1):65–71. https://doi.org/10.1001/2013.jamasurg.2
6. Seesing MFJ et al (2017) A propensity score matched analysis of open versus minimally invasive transthoracic esophagectomy in the Netherlands, (in eng). Ann Surg 266(5):839–846. https://doi.org/10.1097/sla.0000000000002393
7. Akasu T, Takawa M, Yamamoto S, Yamaguchi T, Fujita S, Moriya Y (2010) Risk factors for anastomotic leakage following intersphincteric resection for very low rectal adenocarcinoma. J Gastrointest Surg 14(1):104–111. https://doi.org/10.1007/s11605-009-1067-4
8. Lindner K, Fritz M, Haane C, Senninger N, Palmes D, Hummel R (2014) Postoperative complications do not affect long-term outcome in esophageal cancer patients, (in eng). World J Surg 38(10):2652–2661. https://doi.org/10.1007/s00268-014-2590-3

9. Schmidt HM et al (2017) Defining benchmarks for transthoracic esophagectomy: a multicenter analysis of total minimally invasive esophagectomy in low risk patients," (in eng). Ann Surg 266(5):814–821. https://doi.org/10.1097/sla.0000000000002445
10. van Workum F et al (2017) Improved functional results after minimally invasive esophagectomy: intrathoracic versus cervical anastomosis, (in eng). Ann Thorac Surg 103(1):267–273. https://doi.org/10.1016/j.athoracsur.2016.07.010
11. Struecker B et al (2018) Evaluation of anastomotic leak after esophagectomy for esophageal cancer: typical time point of occurrence, mode of diagnosis, value of routine radiocontrast agent studies and therapeutic options, (in eng). Dig Surg 35(5):419–426. https://doi.org/10.1159/000480357
12. Hagens ERC, Reijntjes MA, Anderegg MCJ, Eshuis WJ, van Berge Henegouwen MI, Gisbertz SS (2021) Risk factors and consequences of anastomotic leakage after esophagectomy for cancer, (in eng). Ann Thorac Surg 112(1):255–263. https://doi.org/10.1016/j.athoracsur.2020.08.022
13. Watanabe M et al (2014) Total gastrectomy risk model: data from 20,011 Japanese patients in a nationwide internet-based database, (in eng). Ann Surg 260(6):1034–1039. https://doi.org/10.1097/sla.0000000000000781
14 Weledji EP (2018) Is patient factor more important than surgeon-related factor in sepsis prevention in colorectal surgery? Int J Surg Open 12:29–36. https://doi.org/10.1016/j.ijso.2018.07.001
15. Sartelli M, Griffiths EA, Nestori M (2015) The challenge of post-operative peritonitis after gastrointestinal surgery, (in eng). Updates Surg 67(4):373–381. https://doi.org/10.1007/s13304-015-0324-1
16 Michelet P et al (2005) Perioperative risk factors for anastomotic leakage after esophagectomy: influence of thoracic epidural analgesia. Chest 128(5):3461–3466. https://doi.org/10.1378/chest.128.5.3461
17 Thornton M et al (2011) Management and outcome of colorectal anastomotic leaks. Int J Color Dis 26(3):313–320. https://doi.org/10.1007/s00384-010-1094-3
18. Whooley BP, Law S, Alexandrou A, Murthy SC, Wong J (2001) Critical appraisal of the significance of intrathoracic anastomotic leakage after esophagectomy for cancer, (in eng). Am J Surg 181(3):198–203. https://doi.org/10.1016/s0002-9610(01)00559-1
19. Mirnezami A, Mirnezami R, Chandrakumaran K, Sasapu K, Sagar P, Finan P (2011) Increased local recurrence and reduced survival from colorectal cancer following anastomotic leak: systematic review and meta-analysis, (in eng). Ann Surg 253(5):890–899. https://doi.org/10.1097/SLA.0b013e3182128929
20. Krarup PM, Nordholm-Carstensen A, Jorgensen LN, Harling H (2014) Anastomotic leak increases distant recurrence and long-term mortality after curative resection for colonic cancer: a nationwide cohort study, (in eng). Ann Surg 259(5):930–938. https://doi.org/10.1097/SLA.0b013e3182a6f2fc
21. Hammond J, Lim S, Wan Y, Gao X, Patkar A (2014) The burden of gastrointestinal anastomotic leaks: an evaluation of clinical and economic outcomes, (in eng). J Gastrointest Surg 18(6):1176–1185. https://doi.org/10.1007/s11605-014-2506-4
22. Tsalikidis C et al (2023) Predictive factors for anastomotic leakage following colorectal cancer surgery: where are we and where are we going?, Curr Oncol 30(3):3111–3137,. [Online]. Available: https://www.mdpi.com/1718-7729/30/3/236.
23. Alverdy JC (2023) Biologically inspired gastrointestinal stapler design: "Getting to Zero" complications, (in eng). Am J Surg 226(1):48–52. https://doi.org/10.1016/j.amjsurg.2023.01.030
24. Dobrin PB (1978) Mechanical properties of arteries, (in eng). Physiol Rev 58(2):397–460. https://doi.org/10.1152/physrev.1978.58.2.397
25. Fung Y-C (1993) Biomechanics - Mechanical Properties of Living Tissues. Springer New York, NY, XVIII, 568
26. Fung YC (1968) Biomechanics. Its scope, history, and some problems of continuum mechanics in physiology., 1 ed. Applied Mechanics Reviews. 1–20.
27. Gregersen H (2003) Biomechanics of the gastrointestinal tract, 1 ed. Springer London, XV, 268
28. Kararli TT (1995) Comparison of the gastrointestinal anatomy, physiology, and biochemistry of humans and commonly used laboratory animals. Biopharm Drug Dispos 16(5):351–380. https://doi.org/10.1002/bdd.2510160502
29. Ripken D, Hendriks HFJ (2015) Porcine Ex Vivo Intestinal Segment Model, in *The Impact of Food Bioactives on Health: in vitro and ex vivo models*, K. Verhoeckx *et al.* Eds. Cham (CH): Springer Copyright 2015, The Author(s). 255–62
30. Russell WMS, Burch RL (1959) The principles of humane experimental technique. Methuen
31. Micheler C (2017) Entwicklung eines automatisierten, druckgeregelten Perfusionsbioreaktors zur Kultivierung von 3D-Zellkulturen. Masterarbeit. Klinikum rechts der Isar, Technische Universität München Munich, Department of Orthopaedics and Sport Orthopaedics
32. Micheler C, Foehr P, Burgkart R (2017) Integration eines Low-Cost Touchscreen Display als Bedienoberfläche für das myRIO-System
33. Micheler C et al (2021) Bioreactor design for the mechanical stimulation by compression of 3D cell cultures. Curr Dir Biomed Eng 7:899–902. https://doi.org/10.1515/cdbme-2021-2229
34 Whalen GE, Harris JA, Geenen JE, Soergel KH (1966) Sodium and water absorption from the human small intestine. The accuracy of the perfusion method, (in eng). Gastroenterology 51(6):975–84
35. Soergel K (1971) Flow measurements of test meals and fasting contents in the human small intestine, Gastrointest Motil 81–92
36. Fordtran JS, Saltin B (1967) Gastric emptying and intestinal absorption during prolonged severe exercise, (in eng). J Appl Physiol 23(3):331–335. https://doi.org/10.1152/jappl.1967.23.3.331
37. Cooper H, Levitan R, Fordtran JS, Ingelfinger FJ (1966) A method for studying absorption of water and solute from the human small intestine, (in eng). Gastroenterology 50(1):1–7
38. Fordtran JS, Locklear TW (1966) Ionic constituents and osmolality of gastric and small-intestinal fluids after eating. Am J Dig Dis 11(7):503–521. https://doi.org/10.1007/BF02233563
39. Fordtran J, Ingelfinger F (1968) Absorption of water, electrolytes, and sugars from the human gut. Handb Physiol Sect 6:1457–1490
40. Schultz SG, Solomon AK (1961) Determination of the effective hydrodynamic radii of small molecules by viscometry. J Gen Physiol 44:1189–1199. https://doi.org/10.1085/jgp.44.6.1189
41. Fink S (1959) The intraluminal pressures in the intact human intestine, (in eng). Gastroenterology 36(5):661–671
42 Painter NS, Truelove SC (1964) The intraluminal pressure patterns in diverticulosis of the colon. I. resting patterns of pressure. II. The effect of morphine, (in eng). Gut 5(3):201–13. https://doi.org/10.1136/gut.5.3.201
43. Shafik A, El Sibai O, Shafik A (2007) Study of the duodenal contractile activity during antral contractions, (in eng). World J Gastroenterol 13(18):2600–2603. https://doi.org/10.3748/wjg.v13.i18.2600
44. Surgery UOIDO, Condon RE, Nyhus LM, Surgery UOIDO, Surgery UOIATMCDO (1972) Manual of Surgical Therapeutics. Little, Brown
45 Cobb WS, Burns JM, Kercher KW, Matthews BD, James Norton H, Todd Heniford B (2005) Normal intraabdominal pressure in healthy adults, (in eng). J Surg Res 129(2):231–5. https://doi.org/10.1016/j.jss.2005.06.015

46. Daristotle JL et al (2019) Improving the adhesion, flexibility, and hemostatic efficacy of a sprayable polymer blend surgical sealant by incorporating silica particles. Acta Biomater 90:205–216. https://doi.org/10.1016/j.actbio.2019.04.015
47. Mann HB, Whitney DR (1947) On a test of whether one of two random variables is stochastically larger than the other. Ann Math Stat 50–60
48. Wilcoxon F (1945) Individual comparisons by ranking methods. Biom Bull, 1, 80–83, ed
49. Fisher RA (1970) Statistical methods for research workers, in *Breakthroughs in statistics: Methodology and distribution*: Springer, 66–70
50. Kelly P (2013) Solid mechanics part ii: Engineering solid mechanics small strain. Univ Auckland
51 Panda SK, Buist ML (2020) A viscoelastic framework for inflation testing of gastrointestinal tissue. J Mech Behav Biomed Mater 103:103569. https://doi.org/10.1016/j.jmbbm.2019.103569
52. Roylance D (2001) Engineering viscoelasticity. Dept Mater Sci Eng-Mass Inst Technol Camb MA 2139:1–37
53 Soffers JHM, Hikspoors JPJM, Mekonen HK, Koehler SE, Lamers WH (2015) The growth pattern of the human intestine and its mesentery. BMC Dev Biol 15(1):31. https://doi.org/10.1186/s12861-015-0081-x
54 Zarnescu E, Zarnescu N, Costea R (2021) Updates of risk factors for anastomotic leakage after colorectal surgery. Diagnostics 11:2382. https://doi.org/10.3390/diagnostics11122382
55. Kang J, Kim H, Park H, Lee B, Lee KY (2022) Risk factors and economic burden of postoperative anastomotic leakage related events in patients who underwent surgeries for colorectal cancer. PLoS One 17(5):e0267950. https://doi.org/10.1371/journal.pone.0267950
56. Goshen-Gottstein E et al (2019) Incidence and risk factors for anastomotic leakage in colorectal surgery: a historical cohort study, (in eng). Isr Med Assoc J 21(11):732–737
57. Hunt SR, Silviera ML (2016) Anastomotic Construction. In: Steele SR, Hull TL, Read TE, Saclarides TJ, Senagore AJ, Whitlow CB (eds) The ASCRS Textbook of Colon and Rectal Surgery. Springer International Publishing, Cham, pp 141–160
58. Man J, Hrabe J (2021) Anastomotic technique-how to optimize success and minimize leak rates, (in eng). Clin Colon Rectal Surg 34(6):371–378. https://doi.org/10.1055/s-0041-1735267